
Transport of particles in Active Galactic Nuclei: study of different numerical approaches

DESY Summer Student Programme, 2014

Simone Garrappa
Università degli studi di Bari, Italy

Elisa Bernardini
Rebecca Gozzini



5th of September 2014

Abstract

In this work a python code to model the time-dependent Synchrotron Self-Compton emission of Active Galactic Nuclei (AGN) is developed. The synchrotron radiation process and the inverse Compton scattering are included, and also a study of different numerical approaches was made in order to reproduce time-dependent phenomena like flaring activity in AGNs.



Contents

1	Introduction	1
2	Active Galactic Nuclei as cosmic accelerators	1
2.1	Synchrotron emission	4
2.2	Inverse Compton Scattering	4
3	Numerical approaches for time-dependent models	5
3.1	The kinetic equation approach	5
3.2	The Fokker-Planck equations approach	8
4	Conclusions	12
5	Acknowledgements	12

1 Introduction

The problem of time-dependent emission in Active Galactic Nuclei consists of interpreting spectral energy distribution of flaring sources. Large flux variability (up to 2 orders of magnitude) is one of the defining properties of blazars, happening on time-scales from years to hours/days. The cause originating flares is currently unknown and must be understood interpreting the electromagnetic emission of these sources with time-dependent models.

Adressed is the problem of connecting the flux variability observed in astronomical data with the possible cause originating it. This includes solving the transport equation, that consists of a system of differential equations for the time evolution of the different particle species present in the source. This equation is generally of the "stiff" type, describing a system with a quick change in time.

In this work, two different models were implemented, with different approaches for modeling the emission processes of particle species in AGNs, the first one is the approach from Mastichiadis & Kirk (1997)[3], and the second is the approach solving the Fokker-Planck equation of Stochastic Acceleration (Park, Petrosian, 1996)[5].

In the first part, there is a quick presentation about AGNs and the two emission processes we consider in our model. In the second part the two different approaches are described and in the last part there are some results from the models developed.

2 Active Galactic Nuclei as cosmic accelerators

The golden decade for astronomy, due in the sixties to the opening of the radio window and the great development of the radio-astronomy research, was characterized of course by the discovery of the microwave background and of pulsars, and by a third great discovery: quasars. The term "quasar" originally stood for "quasi-stellar radio source", and refers to the fact that when an optical telescope is pointed towards the direction of some radio source, which can be as extended as minutes of arc in radio maps, the resulting optical plate shows a source which looks like a star. This "point-like" objects, are instead gigantic energy plants, able to produce much more power than an entire galaxy like the Milky Way, in a volume which is very small, comparable with our Solar System. Interesting outcome that emerged from these observations was that thermonuclear reactions only were not enough to explain the power emitted by quasars.

More informations came with the opening of the X-ray window, in the sixties with rocket experiments (R.Giacconi, B. Rossi) and then with the first X-ray satellites (Uhuru, Ariel 5, HEAO-1, Einstein), in the early seventies. Those experiments made clear that all kinds of quasars were strong X-ray emitters. In the early seventies there were also great improvements of the interferometric technique for radio telescopes, and then was possible to resolve details from sources as close as a few tenths of a millisecond of arc. The first quasars that were discovered were radio-loud, but these are now part (about 10%) of a larger category called Active Galactic Nuclei (AGN). The basic structure of AGNs includes [1]

- *A supermassive black hole*, with $10^6 M_{\odot} < M < 10^{10} M_{\odot}$, most likely spinning, even if we do not have precise measurements of its spin value.
- *An accretion disk*. Matter with even a small amount of angular momentum, attracted by the black hole gravity, spirals in and forms a disk. The accretion disk represents

a major source of power for AGNs.

- *An X-ray corona*, surrounding the accretion disk. It is supposed to be a hot layer, or an ensemble of particularly active regions in the inner parts of the disk.
- *An obscuring torus* located at several parsec from the black hole, intercepting some fraction of the radiation produced by the disk and re-emitting in the infrared range.
- *The Broad Line Region*. It is a region composed of many small clouds at a distance of $\sim 10^{17} - 10^{18}$ cm from the black hole, moving rapidly (~ 3000 km s $^{-1}$). They intercept $\sim 10\%$ of the ionizing radiation of the disk, and re-emit it in the form of lines broadened by doppler shift.
- *The Narrow Line Region*. It is a region analogous to the Broad Line Region but with less dense clouds, moving less rapidly.

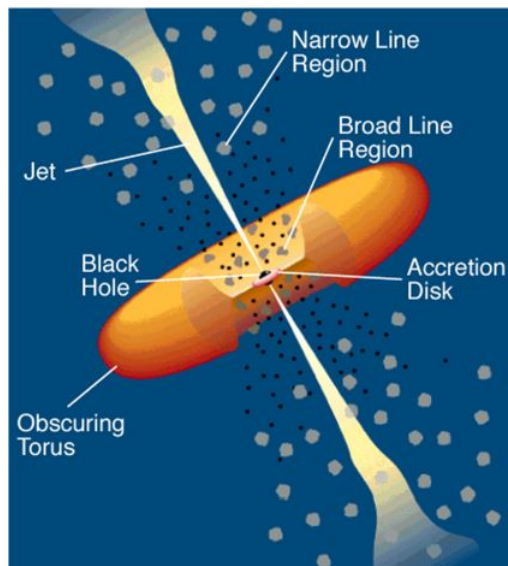


Figure 1: Basic representation of AGN structure.

This is the basic structure of all AGNs, but 10% of them, besides accreting matter, are able to expel it in two oppositely directed *jets*. Their direction likely traces the rotational axis of a spinning black hole. The material inside these jets is moving at relativistic speeds; jets can reach a few Mpc in size, tens of times the radius of their host galaxies. The emission of jets is highly beamed, and their appearance depends on the viewing angle. So these kind of AGNs are classified in two main categories: AGNs whose jets are pointing at us are called *blazars*, and AGNs whose jets are pointing elsewhere are called *radio-galaxies*. The radio emission produced by jets is only a small fraction of the entire electro-magnetic power they emit. We know that most of it is produced in the range of mm-optical and the GeV-TeV band. In turn, the electro-magnetic output is only a small fraction of the total power carried by the jet. Most of it is carried in the form of bulk kinetic energy of the matter flowing relativistically, and by the moving magnetic field; in powerful sources, it reaches the large radio structure: the hot spots and the radio lobes. In less powerful sources,

however, these structures are absent. To distinguish among different kinds of AGNs, we look for their spectra: aligned sources show a *flat radio spectrum* while misaligned sources show a *steep radio spectrum*. The slope of the radio spectrum is thus an indication of the viewing angle.

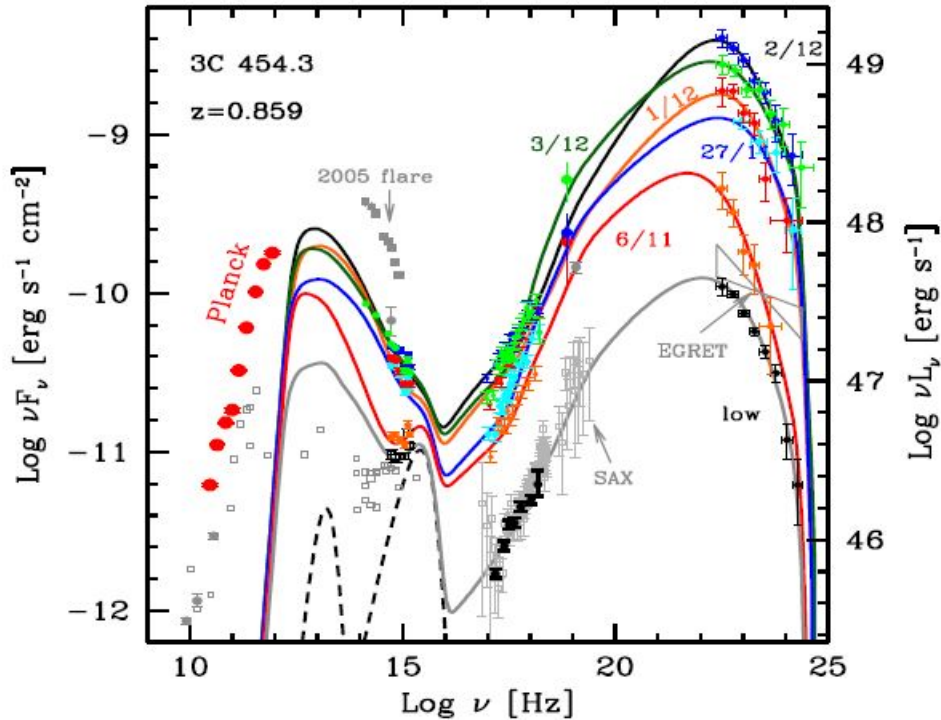


Figure 2: The overall electromagnetic spectrum of 3C 454.3, Dates refer to the year 2009. Lines correspond to fitting models. See Bonnoli et al. (2011,MNRAS,410,368)

As said before, we are interested also in VHE from AGNs, and a good source to take as example is 3C 454.3, that was the brightest blazar detected in the γ -ray band for a few years. In Figure 2 one can see that the observed flux shows a large variability of almost 2 orders of magnitude, both in the γ -ray and in the optical range. Radio sources in general, and blazars in particular, emit over the entire electromagnetic spectrum, from the radio (down to 10^7 Hz) to the TeV band (up to 10^{27} Hz). The overall spectral energy distribution (SED), shows two broad peaks. The location of the peak frequencies varies from object to object, but in general the first peak is between the mm and the soft-X-rays, while the high energy peak is in the MeV-GeV band. It is quite evident from the spectra that they are variable at all frequencies, but especially at high energies. Minimum variability timescales range between weeks and tens of minutes. In restricted frequency ranges, the AGN spectrum is a power law and the high energy peak often dominates the power output. It is rather straightforward to interpret the first peak of the SED as synchrotron emission. Since the flux sometimes varies rapidly and simultaneously (at least in optical-UV-soft-X-rays bands) it is believed that it comes from a single region of the jet. Instead, the high energy peak is believed to be produced by the Inverse Compton process, by the same

electrons producing the synchrotron radiation. The seed photons could be the synchrotron photons themselves (Synchrotron Self Compton) and/or the ambient photons, described previously as broad line/narrow line region. The emissions observed through the whole spectrum, doesn't necessary come from the same region of the AGN, and the SED could be not fully explained with only synchrotron radiation and inverse compton, because especially at VHE we have other non-thermal processes that could be responsible for the emissions (non-thermal brehmsstrahlung, $p - \gamma$ interactions) but they also need a specific enviroment. Synchrotron radiation and inverse compton are always present when we are considering an electron population, so SSC model represents the basic model for reproducing SEDs from radio to VHE band.

2.1 Synchrotron emission

In systems like astrophysical sources, the interaction between relativistic leptons and the magnetic field produces synchrotron radiation. Classical synchrotron emission formulas (Blumenthal Gould 1970) are applied to the case of an initial electron distribution whose direction is isotropic. Considering an emission from many electrons, it is interesting to calculate the *specific emissivity* (power per unit solid angle and per unit frequency produced within a volume of 1 cm^3). In case of an isotropic emission, the specific density is obtained by integrating the single electron emitted power multiplied by the differential electron spectrum:

$$\epsilon_s(\nu) = \int N(\gamma) P_e(\nu, \gamma) d\gamma \quad (1)$$

Synchrotron emission of electrons distributed as a power law with index p produces a photon spectrum in the form of a power law with index α , with the relation:

$$\alpha = \frac{p - 1}{2} \quad (2)$$

2.2 Inverse Compton Scattering

When an electron has energy larger than that of the surrounding radiation, it interacts with the photons via *inverse Compton* scattering, and transfers its energy to the photon, that could gain enough energy to reach the $\gamma - ray$ band. This process is different from the well known Compton scattering, in which the electron is at rest and it is the photon to give part of its energy to the electron.

A complete description of this process is given in [1]. We are interested in some useful considerations as for synchrotron radiation: the spectrum of the scattered photon has typical frequency a factor γ^2 larger than the frequency of the incoming photon [1]. So if we consider the general and realistic case in which the photons are not monochromatic but are distributed in frequency, we have that the inverse Compton emissivity is given by:

$$\epsilon_c(\nu_c) = \frac{1}{4\pi} \frac{(4/3)^\alpha}{2} \frac{\tau_c}{R/c} \nu_c^\alpha \int_{\nu_{min}}^{\nu_{max}} \frac{U_r(\nu)}{\nu} \nu^\alpha d\nu \quad (3)$$

where $U_r(\nu)$ [$\text{erg cm}^{-3} \text{ Hz}^{-1}$] is the specific radiation density at the frequency ν . $U_r(\nu)$ is in general given, at a fixed time t , by:

$$U_r(\gamma, t) = \frac{4\pi}{c} \int_{\nu_{min}}^{\nu_{max}(\gamma)} d\nu I(\nu, t) \quad (4)$$

Where $I(\nu, t)$ is the radiation field measured in [$\text{erg s}^{-1} \text{ cm}^{-2} \text{ sr}^{-1} \text{ Hz}^{-1}$]. More details on integration limits for expressions (3) and (4) are given respectively in [1] and [2].

3 Numerical approaches for time-dependent models

I studied the two approaches adopted in this work to develop a model for time-dependent emissions from AGNs. The first approach is the one adopted in [3] by A. Mastichiadis and J.G. Kirk, and the second is the one adopted in [2] by M. Chiaberge and G. Ghisellini. The main objective was to develop a basic complete SSC model, in order to cover all the electromagnetic spectrum from radio to VHE band, only considering an electrons population interacting with magnetic field and the radiation produced by synchrotron radiation. Then I developed a python[6] code for each method and tested them on numerical stability and response, comparing with known analytical solutions.

3.1 The kinetic equation approach

The Model According to [3], the first approach to model leptonic emission of AGN was to write a kinetic equation in terms of the Lorentz factor γ of the electron, using a normalization in which time is measured in units of the light crossing time of the source (of size R) and the particle density refers to the number contained in a volume element of size $\sigma_T R$ (where σ_T is the Thomson cross section):

$$\frac{\partial n_e(\gamma, t)}{\partial t} = \mathcal{Q}^e(n_e, \gamma, t) + \mathcal{L}^e(n_e, \gamma, t) \quad (5)$$

here \mathcal{L}^e denotes the various electron loss terms while \mathcal{Q}^e are the injection terms. There is no escape term included in the electron equation, since we assume the loss terms to be much larger.

The equation for photons is:

$$\frac{\partial n_\gamma(x, t)}{\partial t} + \frac{n_\gamma(x, t)}{t_{\gamma\text{esc}}} = \mathcal{Q}^\gamma(n_\gamma, x, t) + \mathcal{L}^\gamma(n_\gamma, x, t) \quad (6)$$

where x is the dimensionless photon frequency: $x = h\nu/(m_e c^2)$. Photons leave the source on the timescale $t_{\gamma\text{esc}}$ that is measured in units of the light crossing time R/c . The terms \mathcal{L}^γ and \mathcal{Q}^γ denote the sinks and sources of photons respectively.

A python code for the resolution of the only synchrotron emission case has been developed, setting the electrons kinetic equation with the loss-term[3]

$$\mathcal{L}_{syn}^e = \frac{4}{3} l_B \frac{\partial}{\partial \gamma} [\gamma^2 n_e(\gamma, t)] \quad (7)$$

the term l_B is called "magnetic compactness" defined as:

$$l_B = \left(\frac{U_B}{m_e c^2} \right) \sigma_T R \quad (8)$$

in which $U_B = B^2/8\pi$ is the magnetic energy density and have replaced $\sin^2\theta$ by its average ($= 2/3$) for isotropic electrons.

The source term in the photon equation can be found using the ' δ -function' approximation, in which the emission of a single electron is approximated as monochromatic, so according to [3] the photon source term is:

$$\mathcal{Q}_{syn}^\gamma = \frac{2}{3} l_B b^{-3/2} x^{-1/2} n_e(\sqrt{x/b}, t) \quad (9)$$

Code development With the only inclusion of the synchrotron emission process for electrons, there are two ordinary differential equations to solve simultaneously, one for electrons and one for photons. The approach to the numerical solution is to discretize the variables γ and x , and to integrate the resulting stiff set of coupled ordinary differential equations forwards in time.

The grid chosen for electrons, is equally spaced in the logarithm of γ . For the photons, the grid spacing is in the logarithm of x and is chosen to be twice as large as that in $\log(\gamma)$ for the electrons. Because of the δ -function approximation used, each electron grid point is associated with a single photon grid point. Thus, since the softest and the hardest photons are produced by electron synchrotron radiation only, we take $x_{min} = b\gamma_{min}^2$ and $x_{max} = b\gamma_{max}^2$.

For the integration of the ordinary differential equations, we used a typical method for diffusion equations, a *forward integration method*. The method consists in the discretization of the first order derivative with respect to t , and the equation is solved using Euler's method. The choice to not use a more precise method (i.e. Runge-Kutta methods) to solve the differential equation comes from the discretization of the derivative with respect to γ on the right-hand side of equation is made using the upstream difference, and so it introduce an error that is comparable to the approximation due to the Euler's method, so there is little harm in using it in this case. Discretizing the time variable, if we know the value of n_e or n_γ at every grid point at some time t , then the equation tells us the value at every grid point at time $t+h$, where h is the time-step chosen for the time-grid. In order to iterate on γ and x grids, at fixed time, the best choice was found to be the one from the highest to the lower energy, giving the boundary condition to n_e in γ_{max} .

Code testing The code developed with the kinetic equation approach was only used for synchrotron radiation, because inverse Compton scattering resulted to be numerically unstable in the way the integration of the differential equation was implemented, so it

needs further improvements to become numerically stable and being used for a full SSC model. Nevertheless it proved to be well suitable for modeling synchrotron emission. To check our treatment of synchrotron radiation we injected electrons with a power law spectrum at a constant rate given by:

$$Q^e(\gamma) = Q^e \gamma^{-p} \quad \text{for} \quad \gamma_{min} < \gamma < \gamma_{max} \quad (10)$$

it was also included the photon escape process in the photons equation.

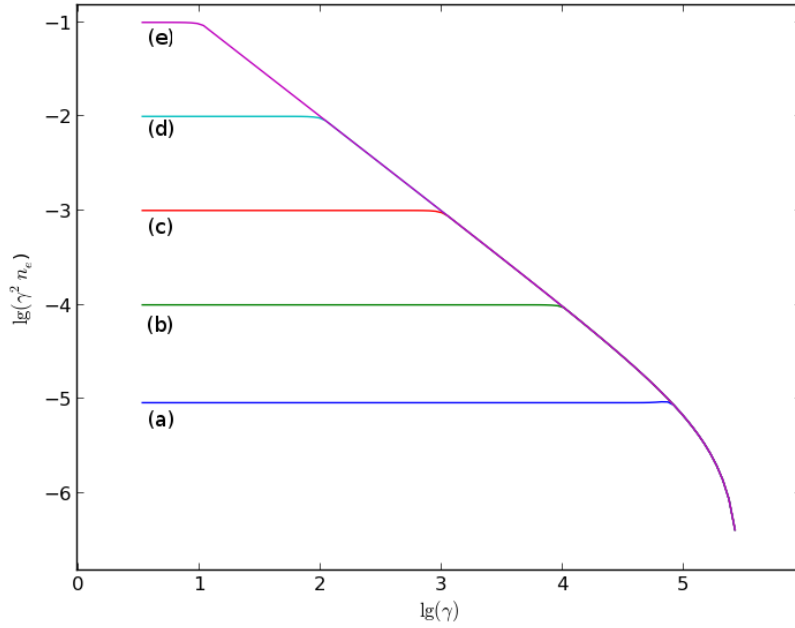


Figure 3: The electron distribution for synchrotron cooling and constant power-law injection. The curves show the evolution of the electron and photon distributions towards steady state. Curve (a) is $t = 10^{-4}$ after electron injection, (b) is for $t = 10^{-3}$, (c) is for $t = 10^{-2}$, (d) is for $t = 10^{-1}$ and (e) is for $t = 1$. All times are expressed in units of t_{cross}

The limits chosen for the electrons energy are $\gamma_{min} = 3$ and $\gamma_{max} = 10^5$. The generated SED are in perfect agreement with analytical solutions (Kardashev 1962). Defining the break point by:

$$\gamma_{br}(t) = \gamma_{max} / (1 + 4\gamma_{max} l_B t / 3) \quad (11)$$

one can clearly see the behavior of the electron distribution in Figure 3, where a power law of index $p = 2$ was chosen and for $\gamma \ll \gamma_{br}$ the electron distribution is approximately a power-law with the same index of the injection term. Whereas for $\gamma \gg \gamma_{br}$ electrons have cooled giving a time-independent spectrum of index $\alpha = p + 1 = 3$.

The photon spectrum in Figure 4 shows a similar behaviour, and the break at high energies

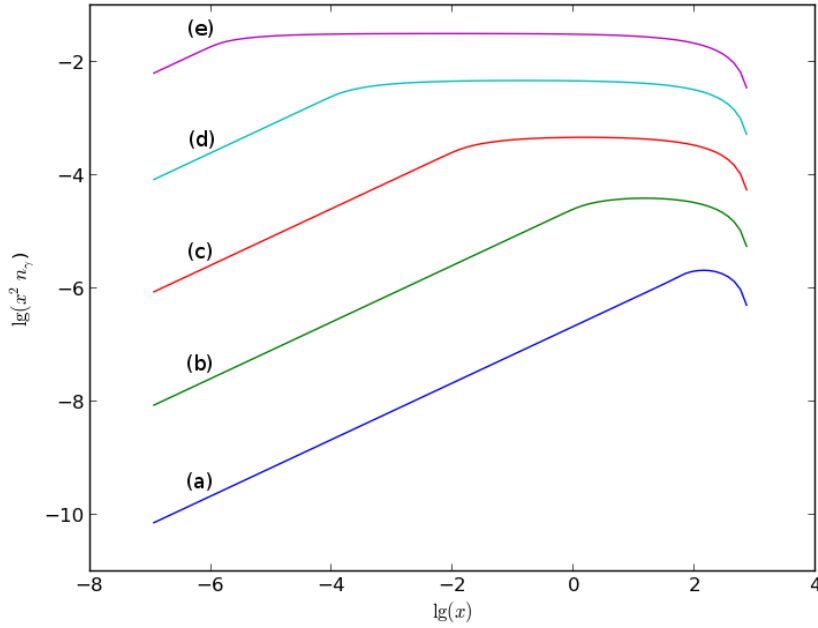


Figure 4: The corresponding photon distribution. Curve (a) is $t = 10^{-4}$ after electron injection, (b) is for $t = 10^{-3}$, (c) is for $t = 10^{-2}$, (d) is for $t = 10^{-1}$ and (e) is for $t = 1$. All times are expressed in units of t_{cross}

x_{br} is related to γ_{br} by $x_{br} = b\gamma_{br}^2$ where in this case we used $b = 10^{-6}$ where $b = B/B_c$ denotes the magnetic field in units of the critical field $B_c = 4.414 \times 10^{13} G$. Photons with $x > x_{br}$ correspond to the 'cooled' part of the electron distribution and have a power law of index $\alpha = 2$. Photons with $x < x_{br}$ have a power law distribution with $\alpha = 1.5$ in agreement with the standard formula (2).

3.2 The Fokker-Planck equations approach

The Model The second method used for developing a model for AGNs emissions was solving the Fokker-Planck equation of stochastic acceleration. As well known in statistical mechanics, the Fokker-Planck equation is a partial differential equation that describes the time evolution of the probability density function of the velocity of a particle under the influence of drag forces and random forces, as in Brownian motion.

In this model, according to [2] is assumed that the emission is produced by a distribution of relativistic electrons injected in a region of typical dimension R embedded in a tangled magnetic field B , at a rate $Q(\gamma) [cm^{-3}s^{-1}]$. Electrons lose energy by emitting synchrotron and synchrotron self-Compton radiation (SSC), and they can also escape from the emitting region on a time-scale t_{esc} , assumed to be independent of energy.

The continuity equation that describes the temporal evolution of the electrons distribution $N(\gamma, t) [cm^{-3}]$ is:

$$\frac{\partial N(\gamma, t)}{\partial t} = \frac{\partial}{\partial \gamma} [\dot{\gamma}(\gamma, t)N(\gamma, t)] + \mathcal{Q}(\gamma, t) - \frac{N(\gamma, t)}{t_{esc}} \quad (12)$$

where $\dot{\gamma} = \dot{\gamma}_S + \dot{\gamma}_C$ is the total cooling rate, given by:

$$\dot{\gamma} = \frac{4}{3} \frac{\sigma_T c}{m_e c^2} [U_B + U_{rad}(\gamma, t)] \gamma^2 \quad (13)$$

where σ_T is the Thomson cross-section, U_B is the magnetic field energy density and $U_{rad}(\gamma, t)$ is the energy density of the radiation field.

Considering the synchrotron and self-Compton radiative losses, we can define the correspondent cooling time-scale:

$$t_{cool} = \frac{3m_e c^2}{4\sigma_T c \gamma (U_B + U_{rad})} \quad (14)$$

Code development As previously said, equation (12) is numerically solved adopting the fully implicit difference scheme of Chang and Cooper (1970)[4] modified for this particular system. The Chang and Cooper scheme allows one to find stable, non-negative and particle-number conserving solutions.

The energy grid used for this purpose, is an equally logarithmic spaced one. The energy meshpoints are defined as:

$$\gamma_j = \gamma_{min} \left(\frac{\gamma_{max}}{\gamma_{min}} \right)^{\frac{j-1}{j_{max}-1}} \quad (15)$$

where j_{max} is the meshpoints number, and the energy intervals are defined as $\Delta\gamma = \gamma_{j+1/2} - \gamma_{j-1/2}$ and the quantities on the right-hand side of the equation are calculated at half grid points. The grids chosen for electrons energy and photon frequency in this simulation contain 200 bins. Following [4], the discretization of the continuity equation is:

$$N_j^i = N(\gamma_j, i\Delta t) \quad (16)$$

$$F_{j\pm 1/2}^{i+1} = \gamma_{j\pm 1/2}^i N_{j\pm 1/2}^{i+1} \quad (17)$$

And so the equation (12) can be written as:

$$\frac{N_j^{i+1} - N_j^i}{\Delta t} = \frac{F_{j+1/2}^{i+1} - F_{j-1/2}^{i+1}}{\Delta\gamma} + \mathcal{Q}_j^i - \frac{N_j^{i+1}}{t_{esc}} \quad (18)$$

We can now rewrite the continuity equation as:

$$V3_j N_{j+1}^{i+1} + V2_j N_j^{i+1} + V1_j N_{j-1}^{i+1} = S_j^i \quad (19)$$

where the V coefficients are

$$V1_j = 0, \quad (20)$$

$$V2_j = 1 + \frac{\Delta t}{t_{esc}} + \frac{\Delta t \dot{\gamma}_{j-1/2}}{\Delta \gamma_j} \quad (21)$$

$$V3_j = -\frac{\Delta t \dot{\gamma}_{j+1/2}}{\Delta \gamma_j} \quad (22)$$

and

$$S_j^i = N_j^i + Q_j^i \Delta t \quad (23)$$

The system of equations (19) forms a tridiagonal matrix, and it is solved numerically using the *solve* function from the *linalg* module in the *numpy* package.

The synchrotron and IC emissivities are then calculated using (1) and (3).

Code testing A complete SSC model was developed with this kind of approach, and it proves to be numerically stable. The main purpose of this kind of model is to reproduce the variability of blazars emission at short time-scale, especially in frequency bands around and above the peaks of blazars SED. During the implementation of the code, several tests were made to verify the behavior of the system reproducing the results obtained with the kinetic equation method, and founding a full agreement with the results obtained about synchrotron emission. The succesfully implementation of the whole synchrotron self-compton model, allows us to cover a wide range of the electromagnetic spectrum. Is thus showed now the case of electrons distributed in energy as a power law $\mathcal{Q}(\gamma) \propto \gamma^{-p}$ with $p = 2$, continuously injected for $t_{inj} \sim R/c$. Input parameters in this case are also $R = 10^{16}$ cm, $\gamma_{min} = 1$, $B = 1$ G, $t_{esc} = 1.5R/c$

In Figure 5 the time-dependent spectra are plotted from $t = R/c$ to $t = 3R/c$. It is interesting is to compare the flux behaviour, after the stop of the injection in the spectral region of the synchrotron peak: one can see that at the highest synchrotron frequencies the decay is very rapid, since the entire source closely follows the decay of the corresponding electron distribution that is shown in Figure 6.

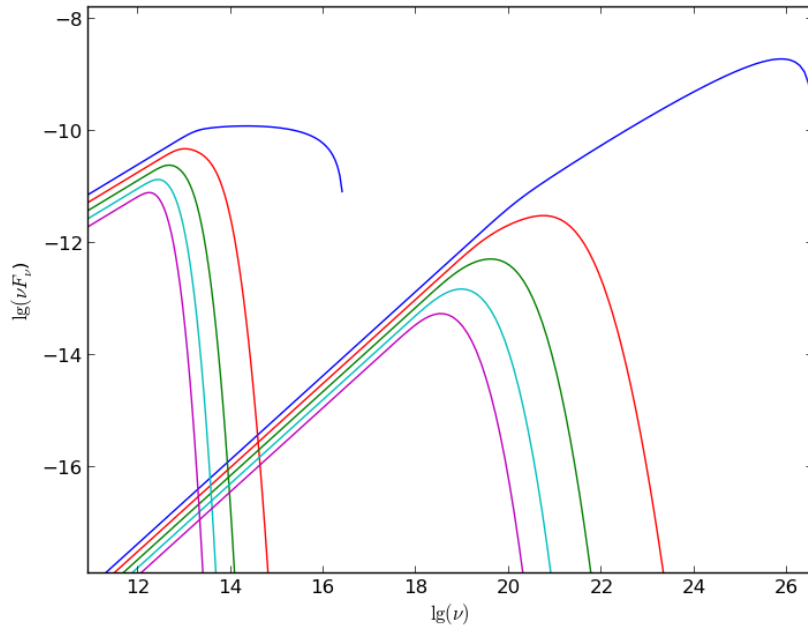


Figure 5: Evolution of the synchrotron self-Compton spectra calculated assuming to inject a power law distribution for $t_{inj} \sim R/c$. The shown spectra are separated in time by $\Delta t = 0.5R/c$. The blue one corresponds to the emission at $t_{inj} = R/c$ when the injection is stopped, and then from red to purple are the cooled spectra forward in time.

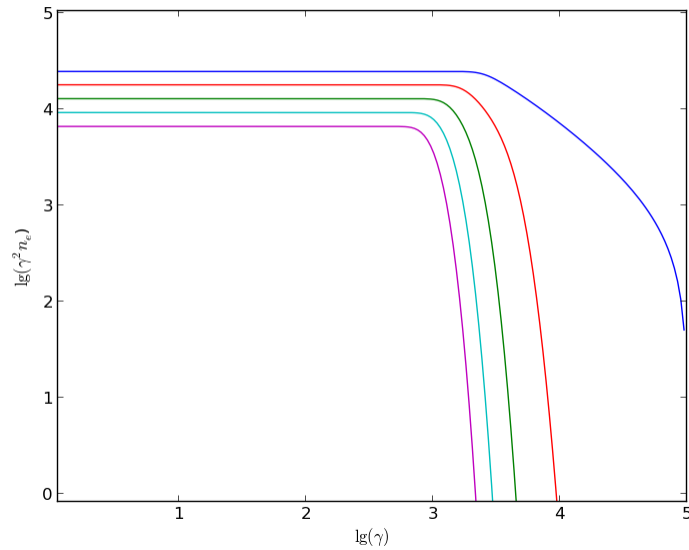


Figure 6: Evolution of the electron spectrum relative to the self-Compton spectra calculated assuming to inject a power law distribution for $t_{inj} \sim R/c$

4 Conclusions

Developing a time-dependent model for emission processes of particle species in AGNs is fundamental for the study and interpretation of flaring events. The SSC model represents the first complete approach to consider the huge range from radio band to VHE band. The implementation of a numerically stable time-dependent SSC model is the main result of this work, that opens to further implementation of this model for the upgrading including other emission processes.

5 Acknowledgements

First of all, I would like to thank my supervisor Rebecca Gozzini for the great enthusiasm she gave to me in this two months challenging this beautiful project, and all the priceless help, support and teachings for which I cannot never thank her enough. I would also like to thank my supervisor Elisa Bernardini, for giving me this opportunity to be here enjoying this so great experience.

Thanks to Karl Jansen to make this summer student experience so good with his infinite kindness and simpaty, I would like to be a theoretical physicist only to have the opportunity to work with you, Karl.

Thanks to Cosimo, for being the best companion in this adventure, and hoping that this was only the first one of many more to come.

Thanks to my companions of the "Astronomers team", Rebecca and Juan Pablo, for the great enthusiasm in sharing this passion.

Finally, I wish to end this with a special thank to my professor Francesco Giordano, for all the support and teachings that I carry on with me everywhere and everytime.

References

- [1] G. Ghisellini, *Radiative processes in high energy Astrophysics*, arXiv:1202.5949v1, (2012).
- [2] M. Chiaberge, G. Ghisellini, *Rapid variability in the synchrotron self-Compton model for blazars*, (1999, MNRAS, 306,551)
- [3] A. Mastichiadis, J.G. Kirk, *Self-consistent particle acceleration in active galactic nuclei* (1997,A&A,320,19)
- [4] Chang J. S.,Cooper G. *A pratical difference scheme for Fokker-Planck equations*, J. Computational Phys., 6,1 (1970).
- [5] B.T. Park,V. Petrosian, *Fokker-Planck equations of stochastic acceleration: a study of Numerical Methods*, (CSSA, 1996)
- [6] *Python programming language official website*, <http://www.python.org>